www.springer.com/41230
https://doi.org/10.1007/s41230-026-4156-z
Research & Development
Vol. 23 No. 4 July 2026
CHINA FOUNDRY

Enhancing forming quality, refining grains, and reducing anisotropy of mechanical properties of WAAM-processed AZ31 alloy by welding torch wobbling

Yi-feng Wang[1, 2, 3], **Zhong-ming Zhang[1, 2, 3], *Chun-jie Xu[1, 2, 3], Wan-ting Xie[1, 2, 3], Yi-bo Xue[1, 2, 3], Shang Sui[1, 2, 3], Can Guo[1, 2, 3], Xiang-quan Wu[1, 2, 3], Sergei Remennik[2, 4], and Dan Shechtman[1, 2, 5]

1. School of Materials Science and Engineering, Xi'an University of Technology, Xi'an 710048, China
2. Xi'an Shechtman Nobel Prize New Materials Institute, Xi'an 710048, China
3. Xi'an Key Laboratory of Advanced Magnesium Alloy Additive Manufacturing and Precision Forming, Xi'an 710048, China
4. Center for Nanoscience & Nanotechnology, Hebrew University of Jerusalem, Edmond J. Safra Campus 91904, Jerusalem, Israel
5. Department of Materials Science and Engineering, Technion-Israel Institute of Technology, Haifa 32000, Israel

Abstract: The arc oscillation has a significant influence on the forming quality and mechanical properties of wire arc additive manufacturing (WAAM) process of magnesium alloy. In order to enhance the forming quality and mechanical properties of WAAM magnesium alloy components, arc oscillation was formed by wobbling welding torch during the process of WAAM with cold metal transfer method, and the impact of various wobble parameters on the formability, microstructure, and mechanical properties of WAAM-processed AZ31 magnesium alloy was studied. The results show that the WAAM-processed AZ31 alloy has a fully equiaxed crystal structure. Wobbling welding torch can increase the effective wall width and significantly improve the forming quality of WAAM. Arc oscillation induced by wobbling welding torch enhances the stirring effect and constitutional supercooling degree of melt pool and accelerates cooling rate of the WAAM-processed AZ31 alloy, therefore the grains in the deposition zone and the heat-affected zone can be refined. Simultaneously, wobbling welding torch significantly enhances the mechanical properties of the WAAM-processed AZ31 alloy. Compared no wobble with a wobble width of 10 mm and length of 4 mm, the grain sizes of the alloy in the deposition zone and heat-affected zone can be reduced by 12.3% and 14.9%, respectively, and the ultimate tensile strength and elongation in building direction increase from 225 MPa and 15% to 239 MPa and 25%, respectively. In addition, anisotropy of mechanical properties between the building direction and the traveling direction is significantly reduced. This study suggests that by adjusting welding torch wobble parameters during the WAAM of AZ31 alloy, it is possible to achieve a synergistic effect that simultaneously enhances the forming quality, reduces the anisotropy of mechanical properties, and improves the mechanical properties of the alloy.

Keywords: AZ31 alloy; wire arc additive manufacturing (WAAM); welding torch wobble; formability; microstructure; anisotropy of mechanical properties

CLC numbers: TG146.22 **Document code:** A **Article ID:** 1672-6421(2026)04-613-11

***Chun-jie Xu**

Ph. D., Professor. His research interests primarily focus on microstructure and property design of high strength and high toughness magnesium alloys, and wire arc additive manufacturing process optimization.

E-mail: xuchunjie@xaut.edu.cn

****Zhong-ming Zhang**

Ph. D., Professor. His research interests mainly focus on magnesium alloy structure optimization and performance control.

E-mail: zmzhang@xaut.edu.cn
Received: 2024-07-24; Revised: 2024-09-16; Accepted: 2024-12-12

1 Introduction

The demand for lightweight materials is increasing with the development of society. Magnesium alloy, as currently the lightest structural metal material in industry, possesses numerous advantages such as high specific strength, high specific stiffness, strong radiation resistance, and high damping capacity[1], making it a promising material for application in various fields such as automotive, electronics, and aviation industry[2]. However, traditional magnesium alloy processing technologies, such as casting, extrusion, and rolling etc., fall short in balancing the production of structural parts with intricate geometries and superior mechanical properties[3]. To further enlarge the industrial application of magnesium alloys, there is an urgent need to develop innovative forming methods[4]. Additive manufacturing, based on the principle of layer-by-layer manufacturing, is an ideal method for fabricating large and complex integral parts due to its high degree of freedom and efficiency[5, 6]. Among the two additive manufacturing methods, wire arc additive manufacturing (WAAM), which based on arc welding process, offers advantages such as high production efficiency, high material utilization rate, low-cost equipment, and cheap production compared to laser metal deposition process[7, 8]. Therefore, WAAM has attracted widespread attention worldwide. Cold metal transfer (CMT) welding technology, characterized by the use of wire feeding to assist droplet transition after the occurrence of short circuits, significantly reduces heat input, minimizes spatter, and stabilizes the arc when applied to WAAM[9]. Consequently, CMT-based wire arc additive manufacturing (CMT-WAAM) exhibits great potential in the additive manufacturing of magnesium alloys[10].

During the CMT-WAAM process of magnesium alloy, process parameters have a significant impact on the microstructure and mechanical properties of parts. Many scholars have attached much importance on the study of WAAM-processed Mg alloys and extensive research has been conducted. Wang et al.[11] deposited a 24-layer thin-wall WE43 magnesium alloy using gas tungsten arc welding additive manufacturing process and found that the microstructure was uneven in the building direction, with the hardness higher at the bottom than at the top. They believed that this uneven microstructure and hardness were attributed to variations in cooling rates among different deposition layers. Yang et al.[12] utilized CMT-WAAM to fabricate a 30-layer AZ31 magnesium alloy thin-wall component, the tensile strength in the travelling direction and building direction was 210.5 MPa and 151.9 MPa, respectively, which indicated a significant anisotropy of mechanical properties in the thin-wall component. Guo et al.[13] deposited magnesium alloy thin-walls using tungsten inert gas welding, the result indicated that pulse frequency can affect both the microstructure and mechanical properties, and the difficulties in controlling the melt pool hindered the achievement of the anticipated forming effects. Xiong et al.[14] found that excessive wire feeding speed reduced the surface quality of a multi-layer single-pass thin-wall when other process parameters were kept constant, whereas the good match of wire feeding speed and welding speed can improve the surface quality of the thin-wall.

Some scholars have introduced arc oscillation in magnesium alloy welding and studied its effects on microstructure and properties. Bi et al.[15] incorporated arc oscillation into CMT technology to produce an AZ91 alloy thin-wall with a width of 19 mm, and the thin-wall exhibited a mixed microstructure of coarse and fine equiaxed grains, high surface flatness, and good forming quality. Yuan et al.[16] studied the effect of arc oscillation on microstructure during magnesium alloy welding, and found that arc oscillation facilitated dendrite fragmentation and the formation of fine equiaxed grains. Cheng et al.[17] fabricated thin-walled WAAM-AZ31 magnesium alloy parts using different oscillation modes. They found that arc oscillation could improve the mechanical properties of the thin-walled parts to some extent. However, they did not conduct an in-depth study on the influence of specific parameters on the forming quality and mechanical properties.

The aforementioned research findings suggest that magnesium alloys produced via arc additive manufacturing generally suffer from problems like subpar forming quality and anisotropic of mechanical properties. Arc oscillation, however, proves beneficial in refining the microstructure, boosting mechanical performance, and enhancing the forming quality during WAAM of magnesium alloys. Regrettably, previous studies merely incorporated arc oscillation into the deposition process, overlooking the fact that optimizing the arc oscillation process parameters can also exert a significant influence on the forming quality and mechanical properties.

Therefore, in the present study, arc oscillation was formed by wobbling welding torch in the process of CMT-WAAM, and the influence of wobble arc parameters on the forming quality, microstructure, and mechanical properties of the WAAM-processed AZ31 magnesium alloy was systematically investigated. This study aimed to enhance both the forming quality and mechanical properties of CMT-WAAM magnesium alloy components while mitigating the anisotropy typically associated with additive manufactured structure.

2 Experiment

2.1 Sample fabrication

Single-pass thin-walled specimens with 25 layers were fabricated by CMT-WAAM using AZ31 wires with a diameter of 1.2 mm. Figure 1 depicts a schematic diagram of the CMT-WAAM system used in this study. As shown in Fig. 1(a), the CMT-WAAM system consisted of a Fox CMT Advance 4000 welding power source, an ABB IRB 2600 robot, a CMT welding torch, a substrate, an argon gas delivery system, and a remote-control operation panel. The substrate material was an AZ31 magnesium alloy with a thickness of 50 mm and dimensions of 300 mm in both length and width, and it was ground and polished to remove the surface oxide layer, and then heated to 160 °C before use. During the CMT-WAAM process, the welding torch remained perpendicular to the substrate, and was wobbling linearly from side to side along arc traveling direction. The single-pass thin-walled specimens with a length of approximately 100 mm and a height of around 70 mm illustrated in Fig. 1(c) were fabricated using the Z-shape wobble mode depicted in Fig. 1(b) and a reciprocating deposition path. The interlayer dwell time was 80 s. Before depositing the subsequent layer, the oxide layer on the surface of the previous layer was removed using a steel brush.

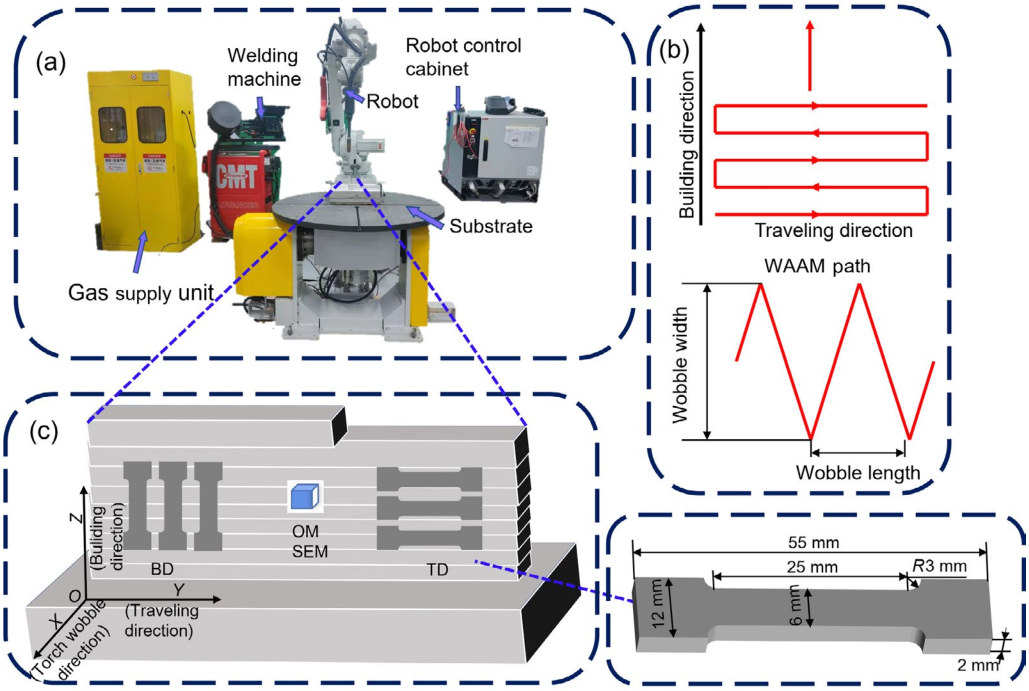

Fig. 1: Schematic diagram of WAAM system and experiment process: (a) hardware composition of CMT-WAAM system; (b) WAAM path and wobble mode of welding torch; (c) multi-layer thin-walled sample, tensile samples, and metallographic sample

To ensure comparability among different specimens, the CMT-WAAM process parameters used for fabricating the thin-walled specimens were kept consistent except for the wobble parameters, i.e. wobble length and wobble width. The specific deposition parameters are shown in Table 1.

2.2 Macroscopic morphology characterization

For the multi-layer thin-walled specimens, a three-dimensional coordinate system was established, as shown in Fig. 1(c). The *X*-axis, *Y*-axis, and *Z*-axis are welding torch wobble direction, traveling direction of the arc, and building direction of the specimens, respectively. The macroscopic morphology was characterized by the total wall width, effective wall width, and the effective wall width ratio. The total wall width referred to the maximum width of the cross-section (*XZ* plane) of the thin-wall specimen. The effective wall width was the distance between two perpendicular tangent lines on the *XZ* plane, representing the maximum width after removing rough uneven surfaces on both sides of thin-wall specimens. The effective wall width ratio was calculated as the ratio of the effective wall width to the total wall width. The total wall width and effective wall width of the thin-walled specimen were measured using a vernier caliper. The measurements were repeated at least three times to obtain an average value.

Table 1: Parameters for WAAM-processed AZ31 alloys

Deposition parameters	Values
Supply current	100 A
Supply voltage	14.3 V
Wire feed speed	9 $m\cdot min^{-1}$
Travelling speed	7 $mm\cdot s^{-1}$
Wire diameter	1.2 mm
Protective gas flow rate	20 $L\cdot min^{-1}$
Substrate temperature	160 °C
Wobble width	0, 6, 8, 10 mm
Wobble length	0, 3, 4, 5 mm

2.3 Microstructure observation

Metallographic sample was cut from the thin-walled specimen using an electrical discharge wire cutting machine, its sampling location is shown in Fig. 1(c). The *XZ* plane of the metallographic sample was mechanically polished and etched for 2–3 s using a solution comprising 1 mL of nitric acid, 4 g of oxalic acid, and 100 mL of distilled water, and then microstructural analysis was conducted using an optical microscope (OM) and a scanning electron microscope (SEM). The grain size was measured using the intercept method based on metallographic photographs, the size and quantity of the second phases were analyzed by using the software ImageJ.

2.4 Mechanical property testing

Utilizing an electrical discharge wire cutting machine, tensile samples were cut from the thin-walled specimens along both traveling direction and building direction. The dimensions and cutting locations of these samples are detailed in Fig. 1(c). Room temperature tensile tests were conducted using a UTM5101X electronic universal testing machine with a test speed of 1 $mm\cdot min^{-1}$. To ensure the reliability and reproducibility of the measurement results, an average value was calculated from three tensile tests conducted under identical conditions. Following the tensile tests, the fracture morphologies were examined by SEM.

3 Results

3.1 Formability

Figure 2 shows the appearance morphology of AZ31 alloy single-pass multi-layer thin-wall formed using a reciprocating deposition path under different wobble parameters, with the corresponding side sectional views of the thin-wall shown on the right. The effective wall section was outlined by the red dashed lines, and the distance between the two inscribed lines represents the effective wall width. Generally, a higher effective wall width ratio indicates the better forming quality of the WAAM-processed AZ31 alloy thin-wall. The corresponding welding torch wobble parameters alongside the total wall width, effective wall width, and effective wall width ratio are listed in Table 2. It is important to note that preliminary experiments show that if the wobble length is less than 3 mm, only an wobble width of less than 8 mm can be accommodated; otherwise, the welding robot may become unstable due to excessive movement speed, which may result in poor formation of AZ31 magnesium alloy thin-walled components. Moreover, as illustrated in Fig. 2(e), if the oscillation length exceeds 4 mm, arc instability may occur, leading to arc interruption and the formation of defects such as voids in thin-walled specimens. Therefore, applying the welding torch wobbling does not ensure that all wobble parameters are suitable for forming multi-layer thin-walled specimens, six groups of representative and effective arc wobbling parameters for successful formation were employed in this study, as listed in Table 2.

As shown in Fig. 2, the side of the thin-walled specimens is uneven when there is no wobble, leading to a small effective wall width and a low effective wall width ratio, with the value of 6.9 mm and 63%, respectively. This indicates that the forming quality of the specimen is poor when there is no wobble. After the wobble is introduced, the side of the thin-walls is flat and smooth. Additionally, the total wall width, effective wall width, and the effective wall width ratio of thin walls vary with increasing wobble width: the effective wall width, and the effective wall width ratio range from 10.1 to 11.4 mm and 86% to 90%, respectively. Compared to the case without wobble, the effective wall width and its percentage are increased at least 46% and 36%, respectively. These results indicate that the surface quality of the thin-wall is significantly improved. Among them, the surface of specimen for Test No. 5 with a wobble length of 5 mm is the roughest and a surface void exists. It can be seen from Table 2 that the effective wall width and effective wall width ratio are the largest for Test No. 6, this means that the optimal forming quality of the thin-walled specimens is achieved when the wobble width is 10 mm and the wobble length is 4 mm in this study.

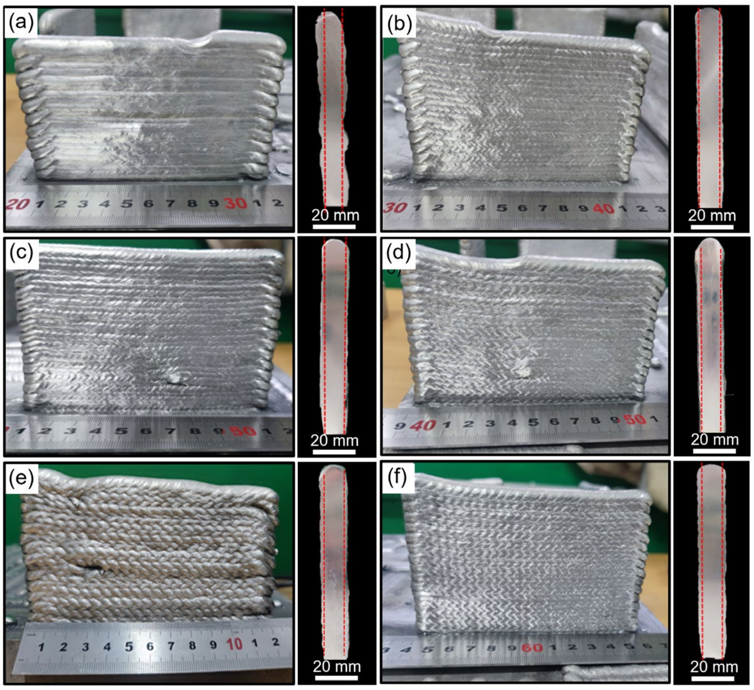

Fig. 2: Photos of thin-wall specimens with different wobble parameters: (a) No. 1; (b) No. 2; (c) No. 3; (d) No. 4; (e) No. 5; (f) No. 6

Table 2: Total wall width, effective wall width, and effective wall width ratio of thin-walled specimens

No.	Wobble width (mm)	Wobble length (mm)	Total wall width (mm)	Effective wall width (mm)	Effective wall width ratio (%)
1	0	0	10.9	6.9	63
2	6	3	11.4	10.1	88
3	8	3	11.9	10.5	88
4	8	4	11.9	10.4	88
5	8	5	11.8	10.1	86
6	10	4	12.6	11.4	90

3.2 Microstructure and phase constitution

For the sake of simplicity and clarity, only the results of No. 1, No. 2, and No. 6 are presented here to observe the changes in the microstructure of the specimens as the wobble length and width increase, as shown in Fig. 3. Figures 3(a–d) are optical microstructures of Specimen No.1 without the wobble of a welding torch, whereas Figs. 3(e–h) and Figs. 3(i–l) depict the corresponding metallographic optical microscope images of Specimens No. 2 and No. 6. It can be observed that regardless of whether the wobble is applied, the overall macroscopic morphologies of the WAAM-processed AZ31 alloy thin-wall specimens are characterized by three zones along the building direction, i.e. the deposition zone (DZ), the remelting zone (RZ), and the heat affected zone (HAZ), which appear cyclically in sequence. The microstructure in each zone is equiaxed grains, but the grain sizes vary among the zones. The RZ zone is located at the bottom of the molten pool, where the grain size is smaller due to the heterogeneous nucleation mode and a relatively high cooling rate. The HAZ undergoes intense heating, resulting in grain growth, with a grain size approximately three times larger than that in the RZ. Among the three zones, the DZ occupies the largest volume fraction, and its grain size is between that of the RZ and the HAZ. It can be seen form Fig. 3 that under all experimental parameters, the heights of RZ and HAZ are approximately the same.

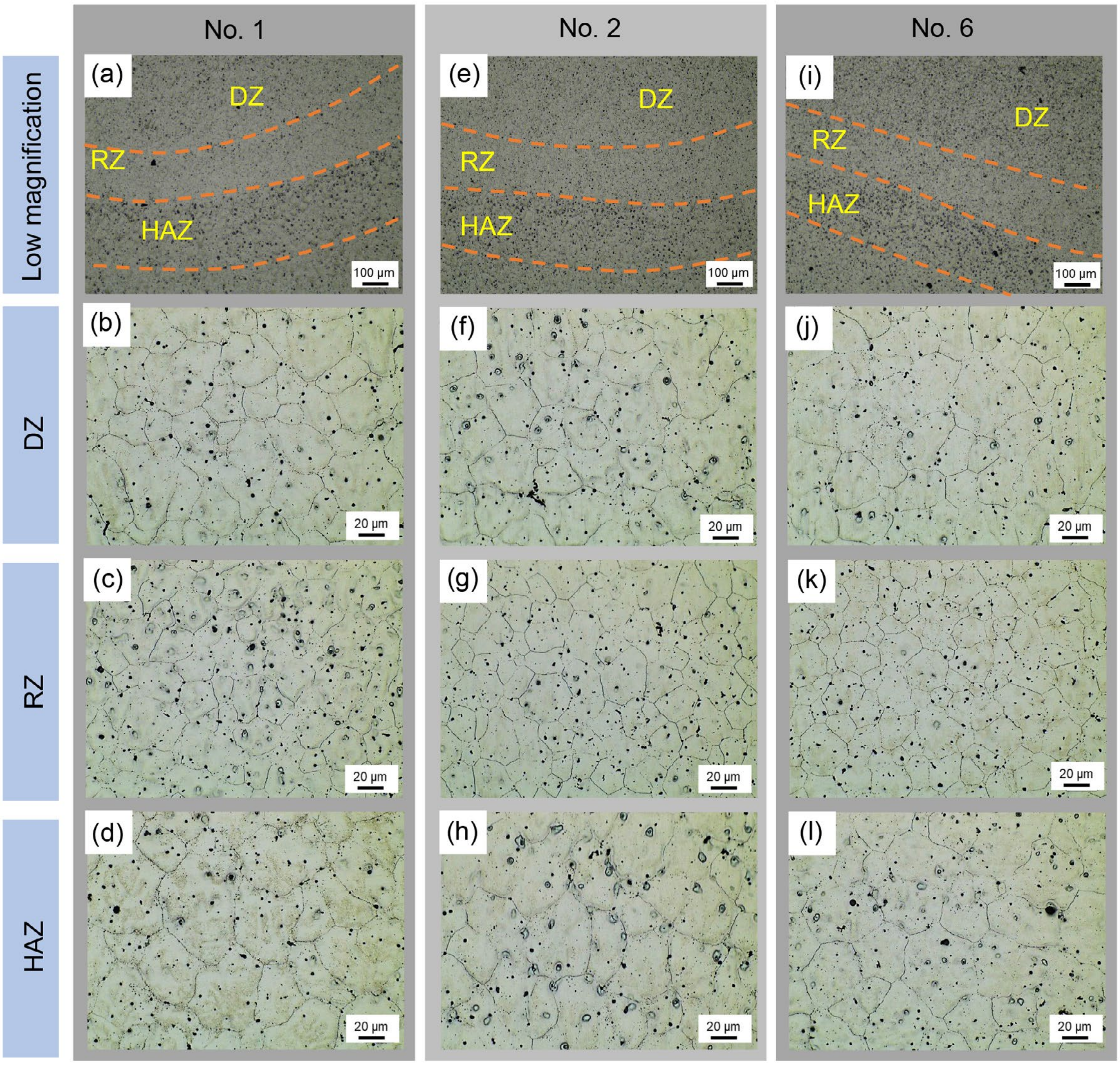

Fig. 3: OM microstructure of WAAM-processed AZ31 alloy thin-wall specimens: (a–d) No. 1; (e–h) No. 2; (i–l) No. 6

In each layer of the thin-walled specimen, the welding torch wobble refines the grain sizes in both the DZ and HAZ zones, although it does not affect the overall macroscopic morphology of the WAAM-processed AZ31 alloys. Based on the grain size measurements summarized in Fig. 4, it is evident that in the absence of welding torch wobble, the grain sizes in the DZ and the HAZ are 42 µm and 71 µm, respectively. When the welding torch wobbled with a width of 10 mm and a length of 4 mm, the corresponding grain sizes are 37 µm and 62 µm, representing reductions of 12% and 13%, respectively. Moreover, when the welding torch has a wobble width of 6 mm and a wobble length of 3 mm, the average grain sizes in the DZ and HAZ are 37 µm and 68 µm, respectively. Whereas, the grain size in the RZ is not affected by the wobble and remains at about 24 µm.

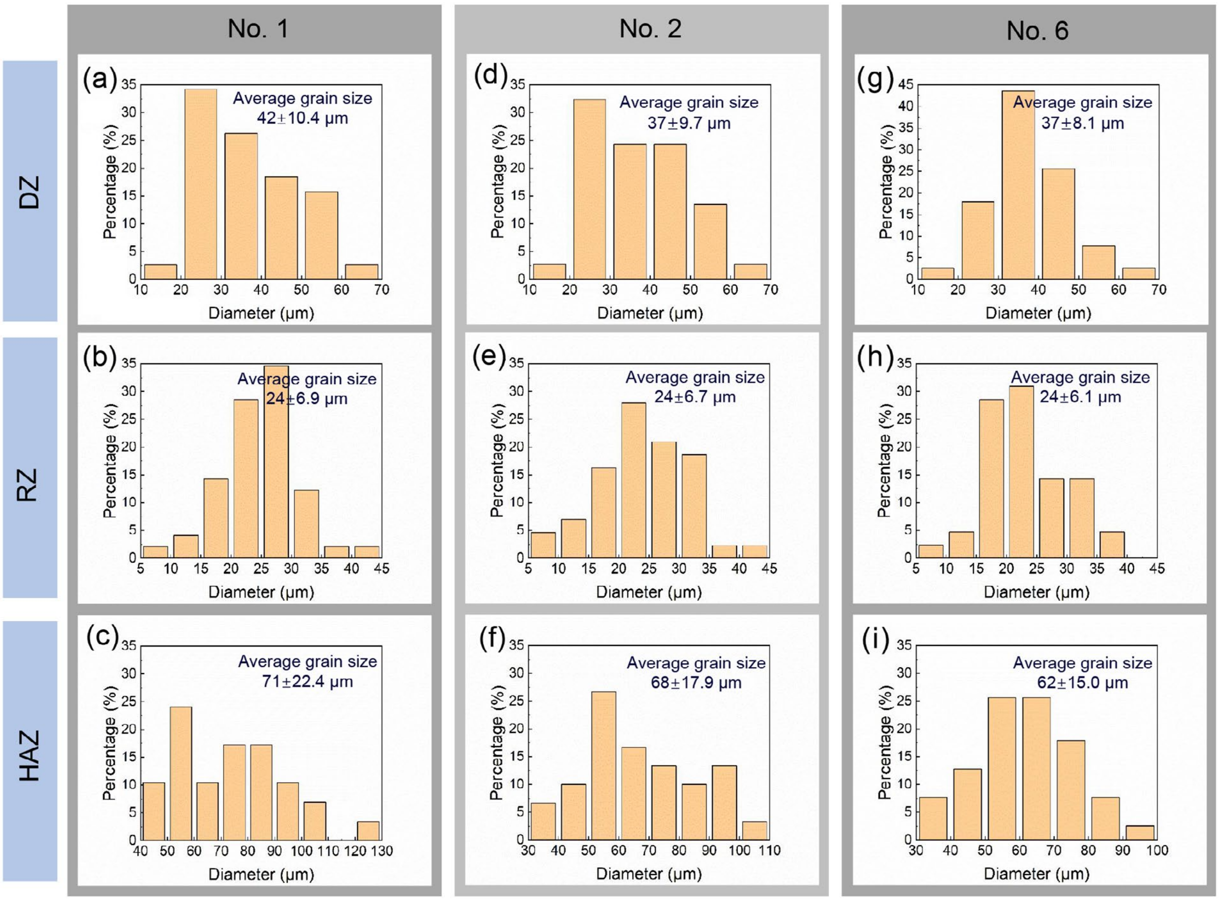

Fig. 4: Grain sizes in different regions of WAAM-processed AZ31 alloy thin-walled specimens: (a–c) No. 1; (d–f) No. 2; (g–i) No. 6

Figure 5 presents the SEM results of the metallurgical structure of AZ31 magnesium alloy thin-walled specimens before and after applying welding torch wobble during the WAAM-CMT process. According to the statistical analysis of the ImageJ, the size, distribution, and quantity of the second phases in specimens with different welding torch wobble parameters are almost identical, and the volume fraction of the second phase is about 0.82%. Therefore, representative No. 1 and No. 6 samples were selected for EDS analysis. An in-depth EDS analysis results of the second phases are presented in Fig. 6. Specifically, at Point 2, the atomic ratio of Al to Mn is approximately 8:5, which is highly consistent with the atomic ratio of Al_8Mn_5. At Points 4 and 7, the main elements are also Al and Mn, and their morphological characteristics are similar to those reported in published literature[12,13,17]; therefore, they are still identified as the Al_8Mn_5 phase. At Points 1 and 6, the atomic ratio of Mg to Al closely resembles that of $Mg_{17}Al_{12}$, leading to the speculation that these regions are composed of $Mg_{17}Al_{12}$. However, at Point 5, despite an excessive Mg content, it is still presumed to be $Mg_{17}Al_{12}$. This deviation may be attributed to the fact that the second-phase particles are smaller than the detection limit of EDS, resulting in the detection of the magnesium matrix along with some additional magnesium elements. At Point 3, it does not closely resemble the atomic ratio of any single phase. It is speculated that the preferential precipitated Al_8Mn_5 serves as a substrate for nucleation of $Mg_{17}Al_{12}$, leading to the formation of a composite phase comprising both Al_8Mn_5 and $Mg_{17}Al_{12}$. This is attributed to the minimal mismatch of only 1.21% between the (111) planes of $Mg_{17}Al_{12}$ and the (111) planes of

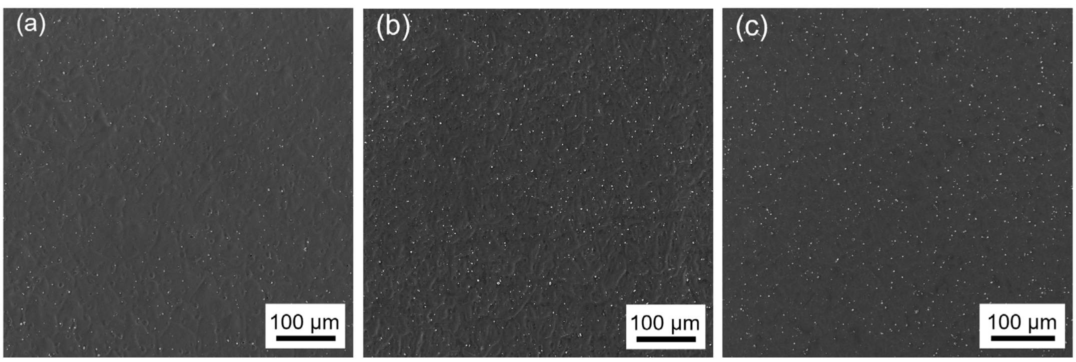

Fig. 5: SEM analysis of WAAM-processed AZ31 alloy thin-walled specimens: (a) No. 1; (b) No. 2; (c) No. 6

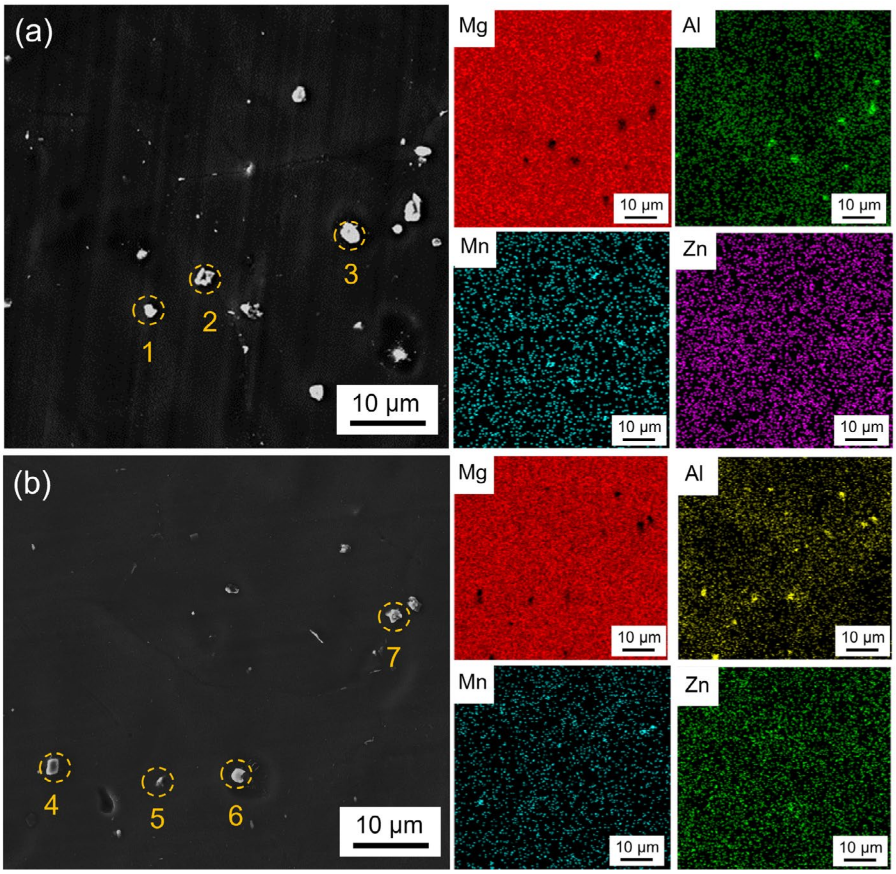

Fig. 6: EDS results of different samples: (a) No. 1 with no wobble; (b) No. 6 with a wobble width of 10 mm and a length of 4 mm

Table 3: EDS point scan results in Fig. 6

Element (at.%)	Point						
	1	2	3	4	5	6	7
Mg	53.05	15.83	32.30	7.79	62.71	56.53	9.03
Al	41.96	47.66	33.24	46.19	29.58	38.96	44.26
Mn	4.20	36.26	34.14	45.89	0.04	0.39	46.60
Zn	0.78	0.25	0.32	0.13	7.67	4.12	0.10

Al_8Mn_5 in AZ31 alloy[18]. In summary, the microstructure of the alloy is composed of a Mg matrix with dispersed large Al_8Mn_5 particles and small $Mg_{17}Al_{12}$ particles. This is consistent with numerous experimental results regarding the CMT-WAAM AZ31 microstructure[12, 13, 18].

3.3 Mechanical properties

Figure 7 illustrates the mechanical properties of WAAM-processed AZ31 alloy thin-walled specimens corresponding to different welding torch wobble parameters outlined in Table 2. Without application of the wobble, the ultimate tensile strength (UTS) of the WAAM-processed AZ31 alloy for No. 1 along building direction (BD) and traveling direction (TD) is 225 MPa and 239 MPa, respectively, with the elongation (EL) of 15% and 20%. Additionally, the yield strengths (YS) are found to be 90.1 MPa and 93.8 MPa, respectively. Notably, the mechanical properties along the TD are superior to those along BD, indicating an anisotropy in mechanical properties, especially for EL.

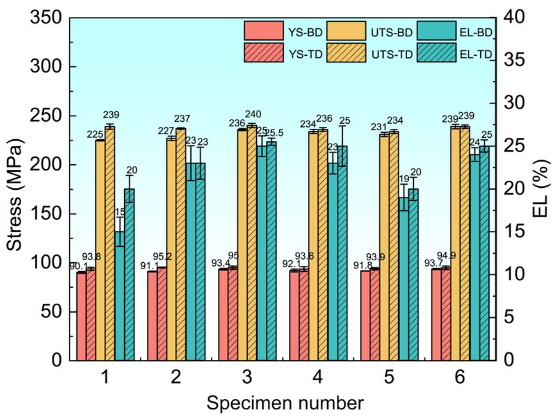

Fig. 7: UTS, YS, and EL of WAAM-processed AZ31 alloys in different directions

After implementing the wobble, it is found that the UTS and YS of the AZ31 alloy fabricated by the WAAM process remain basically consistent in the traveling direction. Moreover, except for the Specimen No. 5, significant improvements in elongation are observed both in BD and TD, and the UTS in BD also increases. When the wobble width was set at 10 mm with a corresponding wobble length of 4 mm (No. 6), the UTS increases from 225 MPa (No. 1) to 239 MPa and the YS increases from 90.1 MPa (No. 1) to 93.7 MPa in BD, which reaches a level equivalent to that in TD of Specimen No. 1. The elongations in BD and TD are similar, being 24% and 25%, respectively. Notably, WAAM with the wobble substantially amplifies the elongation in BD by up to 60%. These findings indicate that the wobble of welding torch significantly reduces the anisotropy of mechanical properties in various directions of the WAAM-processed AZ31 alloy by enhancing both strength and elongation in BD.

As shown in Fig. 7, comparing the Specimen No. 2 with the No. 3 and the Specimen No. 4 with the No. 6 reveals that, for a constant wobble length, increasing the wobble width results in higher UTS and EL, while reducing anisotropy. When comparing the specimen of the No. 3, the No. 4, and the No. 5, with the wobble width keeps constant, an increase in wobble length from 3 mm to 5 mm leads to a decrease in both UTS and EL.

These findings indicate that when the wobble width is 8 mm, a shorter wobble length improves the mechanical properties of thin-walled specimens, with the smallest anisotropy observed at a wobble length of 4 mm. Notably, Specimen No. 6 (with a 10 mm wobble width and a 4 mm wobble length) exhibits an optimal combination of excellent overall mechanical performance and minimal anisotropy.

3.4 Tensile fracture morphologies

Figure 8 illustrates the tensile fracture morphologies of WAAM-processed AZ31 alloys in TD for Specimen No. 1 with no wobble of welding torch and Specimen No. 6 with a wobble width of 10 mm and a length of 4 mm. Both fracture surfaces are composed of dimples and cleavage planes, which indicate that the fracture characteristics are all ductile-brittle fracture mode. A comparison between Fig. 8(b) and Fig. 8(d) indicates that after applying welding torch wobble, the fracture morphology predominantly consists of dimples, with fewer cleavage planes. This alteration aligns with the observed enhancements in elongation in Specimen No. 6.

4 Discussion

4.1 Effect of welding torch wobble on forming quality of CMT-WAAM

Challenges for WAAM may arise from the intricate arc movement trajectory, dynamic heat diffusion, and limited control over the melt pool, which collectively hinder the effective mitigation of the complex disturbances and consequently compromise the stability of the forming process[19]. This instability frequently is prone to cause the formation of various defects, including porosity, weld spatter, and slag inclusions, particularly when inappropriate process parameters or path selection strategies are utilized. Given the layer-by-layer nature of WAAM, the defects progressively accumulate and exacerbate, ultimately impeding the continuity of the forming process[20].

During the WAAM deposition process, wobbling the welding torch can induce arc oscillation, which is helpful to enhance arc stability[21]. As a result, the surface flatness and effective wall width of thin-walled specimens are significantly enhanced. In addition, when the process parameters are poorly matched, excessive deposition heat input in WAAM may cause molten metal to fail to solidify promptly and flow out

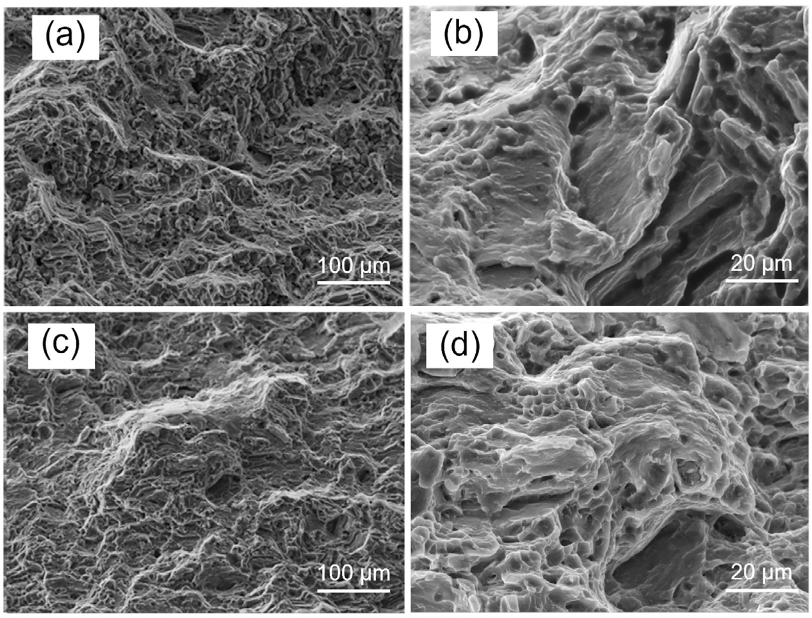

Fig. 8: Tensile fracture morphologies of WAAM-processed AZ31 alloys in traveling direction: (a, b) No. 1 with no wobble; (c, d) No. 6 with a wobble width of 10 mm and a length of 4 mm

freely, which poses a significant challenge to forming process, especially for thin-walled parts. As shown in Fig. 1(b), the CMT-WAAM adopts a zigzag wobble trajectory, the moving speed of welding torch is effectively increased, and consequently heat input is reduced. This technique allows for widening the weld bead without increasing the welding current, thereby improving heat dissipation and preventing melt from flowing freely. As a result, the forming quality of WAAM can be improved.

In conclusion, changing the wobble parameters of welding torch in WAAM can control the morphology of the thin-walled components, expand the process window, and improve forming quality. As a result, it is beneficial for the expanded application of WAAM-processed magnesium alloys.

4.2 Effect of wobble on microstructure of WAAM-processed AZ31 alloys

4.2.1 Formation of solidified structure

In accordance with the criterion for constitutional undercooling, the degree of constitutional undercooling at the front of solidification interface is dependent on the ratio of the temperature gradient G to the solidification velocity R, i.e. G/R, when the chemical compositions of materials are fixed. The small temperature gradient G and high solidification velocity R are conducive to generating constitutional undercooling[8].

During WAAM process, as melt pool solidifies, columnar dendritic grains that approximately perpendicular to the melt pool boundary are formed initially by epitaxial crystallization on the melting boundary at the bottom of melt pool. As arc moves and melt pool further solidifies, G in melt pool becomes smaller in both the building direction and traveling direction, while R becomes higher. Simultaneously, thermal accumulation caused by the multi-layer depositions further reduces G, leading to a further decrease in G/R[22]. Low G/R facilitates the creation of a sufficient constitutional undercooling, leading to the formation of new crystal nuclei in the liquid and the occurrence of columnar to equiaxed transition. Consequently, solidification mode of melt pool changes from epitaxial growth to endogenous growth, and the crystal morphology transforms from columnar dendritic grains to equiaxed dendritic grains. Besides, the convection of melt caused by arc pressure and Marangoni effect in melt pool leads to the disintegration of dendritic grains, and the convection may also cause some grains in the partially melted zone to detach[17]. The free-floating crystals formed by detached grains and dendritic fragments are carried into the melt pool by convection, and they may form the seeds of grains that subsequently grow freely in the melt[16]. Based on the above crystal nucleation and growth process, all the AZ31 thin-walled specimens produced using CMT-WAAM technology solidify with an equiaxed structure.

When depositing multi-layer thin-walls, each subsequent layer is deposited on the top of the preceding layer, thus a DZ is created. Simultaneously, the upper part of the preceding layer is remelted because of the high temperature caused by deposition of the subsequent layer. After the remelted part is solidified, it forms a RZ, and the unmelted part of the preceding layer constitutes the HAZ.

4.2.2 Effect of wobble on solidification process

The implementation of welding torch wobble during CMT-WAAM process has a significant impact on solidification process of alloys. Firstly, wobbling welding torch during the WAAM process can induce arc oscillation and enhance stirring effects within the molten pool[17]. The greater the wobble amplitude, the stronger the stirring effect. The enhanced stirring effect causes more disintegration of dendrites, and thereby promoting the formation of finer equiaxed grains in the deposition zone.

Secondly, wobbling welding torch can increase the cooling rate of molten pool and also contribute to grain refinement. To analyze the cooling rate using the heat conduction rate equation, namely Fourier's Law, the fundamental equation is[23]:

$$q=-\lambda\frac{\mathrm{d}T}{\mathrm{d}x} \tag{1}$$

where, q is the heat flux density, λ is the thermal conductivity of the material, and $\mathrm{d}T/\mathrm{d}x$ is the temperature gradient. It can be inferred that, under constant conditions, a larger heat dissipation area and a higher temperature gradient both contribute to a faster heat dissipation rate. As shown in Fig. 9 and Table 2, welding torch wobble increases the wall width of the specimens, thereby increasing the cross-sectional area of thermal dissipation. This enlarged thermal transfer area increases the heat dissipation rate along the building direction, and weakens the grain growth in the HAZ. Additionally, as the distance between the molten pool boundary and the heat source decreases, the temperature gradient in front of the solid-liquid interface increases[24], leading to an increase in heat flux density, i.e., the cooling rate. Consequently, the grain size in the HAZ is reduced.

4.3 Effect of wobble on mechanical properties

The mechanical properties of the traditionally WAAM-processed thin-walled specimens exhibit significant anisotropy[25]. Whereas, incorporating welding torch wobble during the WAAM process enhances the mechanical properties of the specimen in the building direction and reduces the anisotropy in its mechanical properties, as shown in Fig. 7. The reason of this enhancement can be analyzed as follows. Firstly, the application of the wobble results in finer grain sizes in DZ and HAZ. Grain refinement can not only improve the elongation of the specimens, but also enhance their strength, especially in the building direction. The contribution of fine grain strengthening in the HAZ can be analyzed using Hall-Petch relationship as follows:

$$\sigma_s=\sigma_0+kD^{-0.5} \tag{2}$$

where, σ_s represents the yield stress, σ_0 is the frictional stress on the slip plane during dislocation motion, k is the Hall-Petch constant, and D is the average grain size. According to Ref. [26], σ_0 is 78 MPa, and k ranges from 280 to 320 MPa·μm$^{-0.5}$. The

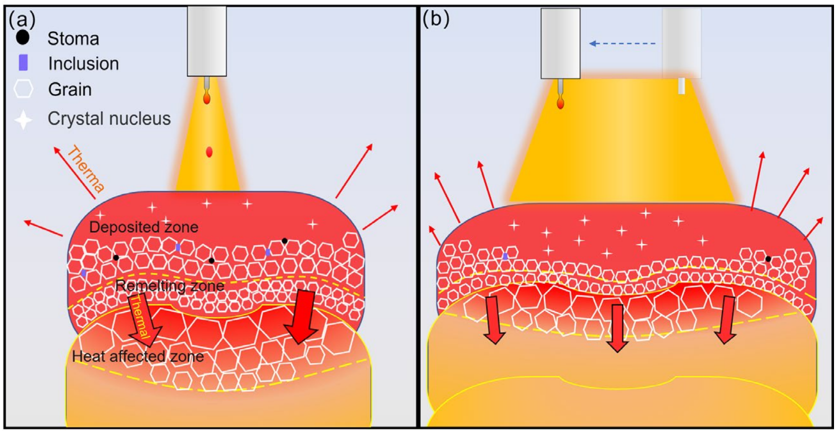

Fig. 9: Influence of wobble on solidification of WAAM deposition process: (a) specimen without arc wobbling; (b) specimen with arc wobbling

grain size in the HAZ in the coarse-grained region decreases from 72 μm in the Specimen No. 1 to 68 μm in the Specimen No. 2 and 61 μm in the Specimen No. 6; the yield stress in the building direction increases by 0.94 MPa and 2.86 MPa, respectively. The measured yield strength in the building direction for the Specimen No. 6 and the Specimen No. 2 is higher by 1.0 MPa and 3.6 MPa compared to the Specimen No. 1, indicating that grain refinement is the dominant factor enhancing the mechanical performance in the building direction, although other strengthening contributions are also present. Secondly, porosity in WAAM-processed alloys in building direction is often unevenly distributed and leading to porosity aggregation[27], which has significantly adverse impact on the mechanical performance of parts[28]. Arc oscillation induced by the wobbling welding torch improves the stability of arc and makes the WAAM forming process more stable, which is beneficial for improving forming quality and mechanical properties. Thirdly, arc oscillation significantly increases the cooling rate, leading to a reduction in dendrite arm spacing and thus refining the microstructure. This refinement further contributes to improved mechanical properties, particularly in building direction.

Overall, implementing welding torch wobble during WAAM processing results in refined microstructures, enhanced arc stability, and improved forming quality. These factors collectively contribute to improved mechanical properties of AZ31 alloy in building direction and a decrease in anisotropy, ultimately enhancing its engineering mechanical performance.

5 Conclusions

(1) During CMT-WAAM process, the application of welding torch wobble significantly enhances both the forming quality and effective wall width of thin-walled AZ31 magnesium alloys. The total wall width, effective wall width, and the percentage of effective wall width of the thin walls all increases with the increase in the wobble width. The optimal forming quality is achieved when the wobble width is 10 mm and the wobble length is 4 mm.

(2) The microstructure of the CMT-WAAM-processed AZ31 alloys exhibits a fully equiaxed grain structure. Under repeated thermal cycles, three distinct grain size zones are formed, i.e. the deposition zone, remelted zone, and heat-affected zone. Welding torch wobble facilitates adequate stirring of the melt pool and promotes constitutional supercooling, resulting in grain refinement. Compared no wobble with a wobble width of 10 mm and length of 4 mm, the grain sizes in deposition zone and heat-affected zone are decreased by 12.3% and 13.9%, respectively.

(3) Optimal performance is achieved with a wobble width of 10 mm and length of 4 mm, resulting in ultimate tensile strength and elongation of 239 MPa and 24% along building direction, respectively. This represents a 6.2% and 60% improvement compared to that with no welding torch wobble, and the mechanical properties along building direction are comparable to those along travelling direction. Within a specific range, adjusting welding torch wobble parameters can improve mechanical properties and reduce anisotropy along the building direction and traveling direction of WAAM-processed AZ31 alloys.

Acknowledgments

The authors would like to acknowledge the support from the Natural Science Basic Research Program of Shaanxi (2023-JC-YB-412), the International Science and Technology Cooperation Program of Shaanxi Province (2023-GHZD-50), the Project of Qin Chuangyuan “Scientist+Engineer” Team Construction, the Key Research and Development Plan of Shaanxi Province (S2023-YF-QCYK-0001-237), the Project of Major Innovation Platforms for Scientific and Technological and Local Transformation of Scientific and Technological Achievements of Xi’an (20GXSF0003), the Project of Major Scientific and Technological Achievements Local Transformation of Xi’an (2022JH-ZDZH-0039), the Scientific Research Program Funded by Shaanxi Provincial Education Department (22JK0479), the Natural Science Foundation of Shaanxi Province (2023-JC-QN-0573), and the Science and Technology Plan Project of Xi’an (2022JH-RYFW-0026).

Conflict of interest

The authors declare that they have no known competing financial interests or personal relationships that could have appeared to influence the work reported in this paper.

References

[1] Zhu T, Chen Z W, Gao W. Incipient melting in partially melted zone during arc welding of AZ91D magnesium alloy. Materials Science and Engineering: A, 2006, 416(1–2): 246–252.
[2] Liao J, Yamamoto N, Nakata K. Gas tungsten arc welding of fine-grained AZ31B magnesium alloys made by powder metallurgy. Materials & Design, 2014, 56: 460–467.
[3] Zhang H, Hu S, Wang Z, et al. The effect of welding speed on microstructures of cold metal transfer deposited AZ31 magnesium alloy clad. Materials & Design, 2015, 86: 894–901.
[4] Yang Y, Xiong X M, Chen J, et al. Research advances in magnesium and magnesium alloys worldwide in 2020. Journal of Magnesium and Alloys, 2021, 9(3): 705–747.
[5] Liberini M, Astarita A, Campatelli G, et al. Selection of optimal process parameters for wire arc additive manufacturing. Procedia CIRP, 2017, 62: 470–474.
[6] Zhang Y, Wu S, Cheng F. A duplex stainless steel (DSS) with striking tensile strength and corrosion resistance produced through wire arc-additive manufacturing (WAAM) using a newly developed flux-cored wire. Materials Letters, 2022, 313: 131760–131765.
[7] Nikam P P, Arun D, Ramkumar K D, et al. Microstructure characterization and tensile properties of CMT-based wire plus arc additive manufactured ER2594. Materials Characterization, 2020, 169: 110671–110684.
[8] Sui S, Guo S, Ma D, et al. Additive manufacturing of magnesium and its alloys: Process-formability-microstructure-performance relationship and underlying mechanism. International Journal of Extreme Manufacturing, 2023, 5(4): 042009.
[9] Zhang B W, Wang C, Wang Z H, et al. Microstructure and properties of Al alloy ER5183 deposited by variable polarity cold metal transfer. Journal of Materials Processing Technology, 2019, 267: 167–176.
[10] Chen F K, Cai X Y, Dong B L, et al. Effect of process modes on microstructure and mechanical properties of CMT wire arc additive manufactured WE43 magnesium alloy. Journal of Materials Research and Technology, 2023, 27: 2089–2101.
[11] Wang Q, Wu G, Tong X. An investigation into wire arc additive manufacturing of Mg-Y-RE-Zr alloy. Materials Letters, 2022, 326: 132922.
[12] Yang X, Liu J, Wang Z, et al. Microstructure and mechanical properties of wire and arc additive manufactured AZ31 magnesium alloy using cold metal transfer process. Materials Science and Engineering: A, 2020, 774: 138942–138951.
[13] Guo J, Zhou Y, Liu C, et al. Wire arc additive manufacturing of AZ31 magnesium alloy: Grain refinement by adjusting pulse frequency. Materials (Basel), 2016, 9(10): 823–837.
[14] Xiong J, Li Y, Li R, et al. Influences of process parameters on surface roughness of multi-layer single-pass thin-walled parts in GMAW-based additive manufacturing. Journal of Materials Processing Technology, 2018, 252: 128–136.
[15] Bi J, Shen J Q, Hu S S, et al. Microstructure and mechanical properties of AZ91 Mg alloy fabricated by cold metal transfer additive manufacturing. Materials Letters, 2020, 276: 28185–128189.
[16] Yuan T, Luo Z, Kou S. Grain refining of magnesium welds by arc oscillation. Acta Materialia, 2016, 116: 166–176.
[17] Cheng S X, Liu F C, Xu Y, et al. Effects of arc oscillation on microstructure and mechanical properties of AZ31 magnesium alloy prepared by CMT wire-arc directed energy deposition. Materials Science and Engineering: A, 2023, 864: 144539.
[18] Pan F S, Feng Z X, Zhang X Y, et al. The types and distribution characterization of Al-Mn phases in the AZ61 magnesium alloy. Procedia Engineering, 2012, 27: 833–839.
[19] Lu Z Y, Tian H Y, Chen S J, et al. Research progress on precision control of arc additive and subtractive composite manufacturing. Acta Metallurgica Sinica, 2020, 56(1): 83–98. (In Chinese)
[20] Strano G, Hao L, Everson R M, et al. Surface roughness analysis, modelling and prediction in selective laser melting. Journal of Materials Processing Technology, 2013, 213(4): 589–597.
[21] Lee T H, Kang M, Oh J H, et al. Deposition quality and efficiency improvement method for additive manufacturing of Ti-6Al-4V using gas metal arc with CMT. Journal of Materials Processing Technology, 2022, 308: 117720.
[22] Gao Z N, Wang L L, Li X, et al. Research on the influence of thermal cycling and temperature gradient on the solidification structure of the molten pool in laser wire additive manufacturing of 7075 aluminum alloy. Chinese Journal of Mechanical Engineering, 2024, 60(1): 96–118.
[23] Varuvel E G, Sonthalia A, Aloui F, et al. Chapter 1 – Basics of heat transfer: Conduction. Handbook of Thermal Management Systems, Elsevier, 2023. https://doi.org/10.1016/B978-0-443-19017-9.00003-9.
[24] Kou S. Welding metallurgy (second edition). John Wiley & Sons, Inc., New York, 2003.
[25] Gu J, Gao M, Yang S, et al. Microstructure, defects, and mechanical properties of wire + arc additively manufactured Al-Cu4.3-Mg1.5 alloy. Materials & Design, 2020, 186: 108357.
[26] Fang X W, Yang J N, Jiang X, et al. Wire-arc directed energy deposited high-performance AZ31 magnesium alloy via a novel interlayer hammering treatment. Materials Science and Engineering: A, 2024, 889: 145864. https://doi.org/10.1016/j.msea.2023.145864.
[27] Li X Z, Zhang M G, Fang X W, et al. Improved strength-ductility synergy of directed energy deposited AZ31 magnesium alloy with cryogenic cooling mode. Virtual and Physical Prototyping, 2023, 18(1): e2170252.
[28] Shen J, You G Q, Long S Y, et al. Abnormal macropore formation during double-sided gas tungsten arc welding of magnesium AZ91D alloy. Materials Characterization, 2008, 59(8): 1059–1065.